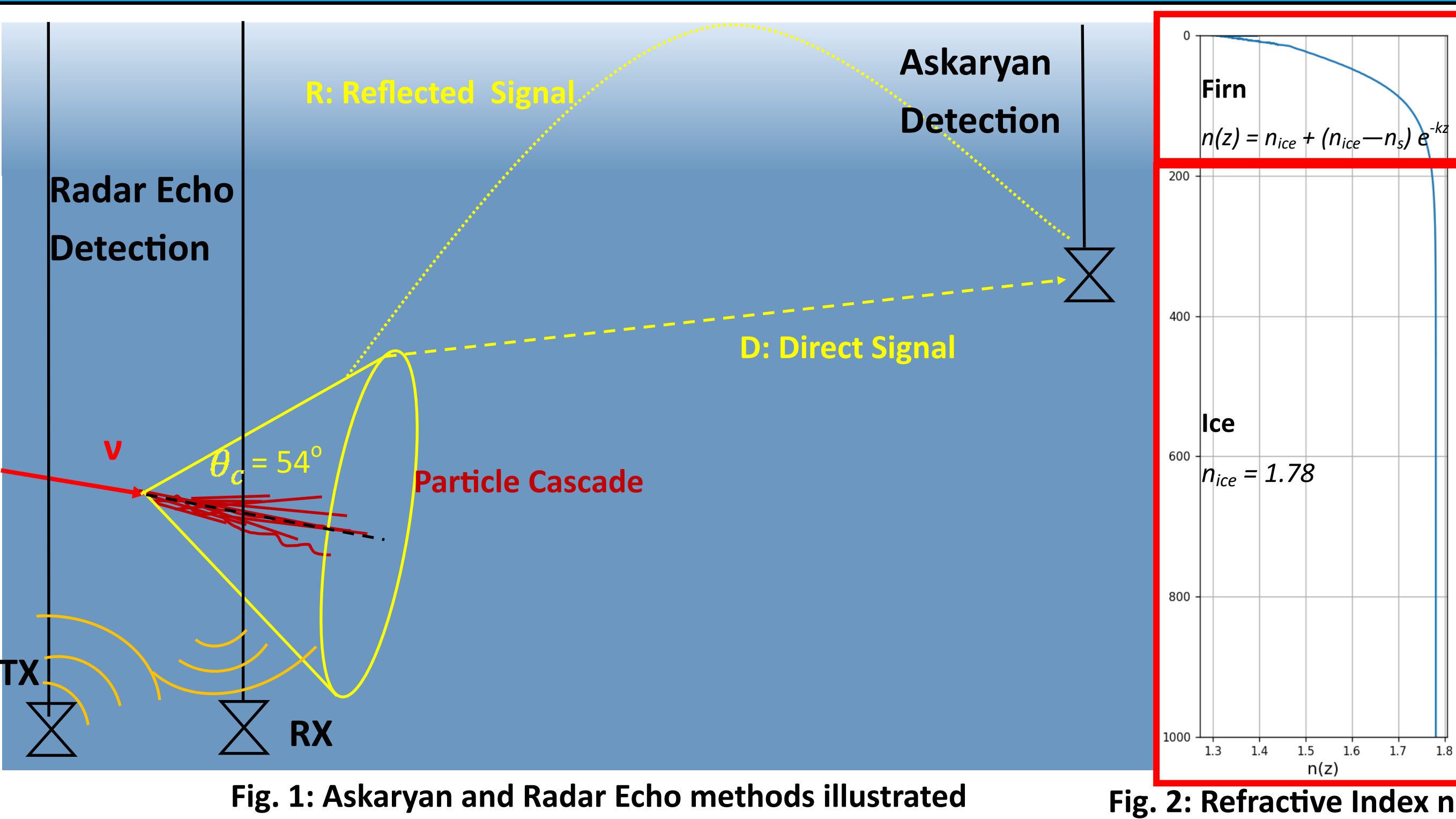


Evolving polar ice and its consequences for radio UHE neutrino detection

Alex Kyriacou* on behalf of the Radar Echo Telescope (RET) Collaboration
 Department of Physics and Astronomy, University of Kansas, Lawrence KS, USA
 Contact at akiriacou@ku.edu



Introduction: Radio Detection of UHE-ν in Ice



Polar ice-sheets are transparent to high frequency radio-waves: 0.1 - 1 GHz ($L_{\alpha} = 992 \pm 121$ m at 0.2 GHz) [4] → Making them ideal detection media for ultra high energy neutrinos (UHE-ν) $E_{\nu} > 10$ PeV, via:

Askaryan effect: Coherent radio emission from charge excess in the relativistic particle cascade [1], *In-Ice Askaryan experiments deploy antennas in the upper 100 m—200 m of polar ice sheets* (Fig. 1) → within or just below the firn layer (Fig 2) Examples: RICE, ARA, ARIANNA, RNO-G, IceCube-Gen2 Radio (proposed)

Radar-Echo effect: Ionization trail persists for a brief time after UHE-ν cascade, acts as a reflective object for in-ice radar (Fig 1.). Effect verified in the lab [13] and is currently being tested in the field using UHE cosmic rays: Radar Echo Telescope for Cosmic Rays (RET-CR) → deployed within upper 15 m of firn [2] Verification of Radar-Echo method will facilitate future development of RET-Neutrino [14]

The firn layer is a dynamic medium with significant temporal fluctuations in density and temperature above 15 m i.e. 'shallow firn'. We present a simulation study to quantify the modulation of RF signals due to evolving ice → The ice-sheet at Summit Station, Greenland (3250 m a.s.l) is used in this analysis

Seasonal Variation in Firn Density

Firn: the transition layer between surface snow and deep glacial ice [12]. Its density increases with depth:
 $\rho(z) = \rho_{ice} + (\rho_{ice} - \rho_s) e^{-kz}$ → Refractive Index is proportional to density: $n(z) = 1.0 + 0.845 \rho(z)$ [6].

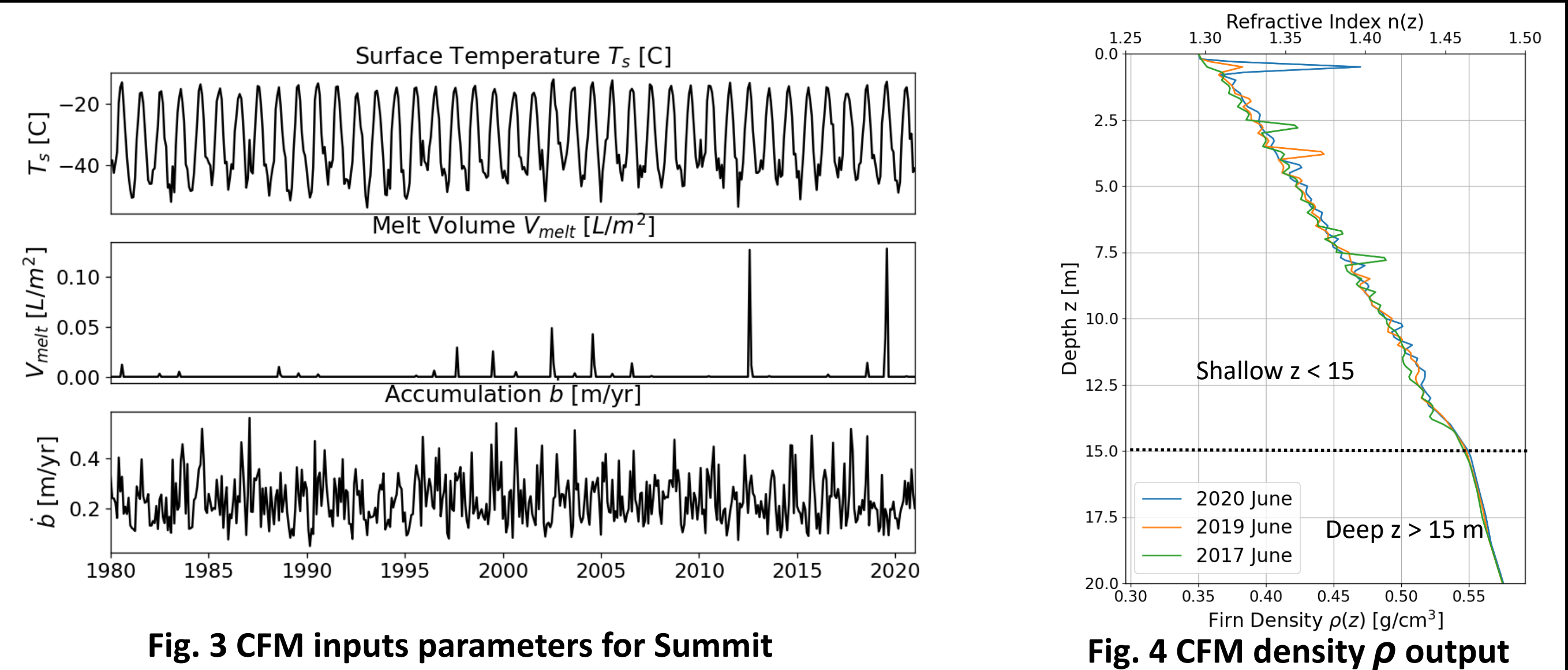
- Random density fluctuations due to changing surface temperature
- Formation of refrozen ice layers due to surface melting events (and rainfall in 2021!)

Summit firn is simulated with the Community Firn Model (CFM) [3] for each month from 1980 to 2020:

Inputs: Surface Temperature, Melt Events, Accumulation Rate, etc. (Fig. 3) - **Output:** Density ρ

Density Fluctuations $\Delta \rho$ for 2000—2020 (Examples for June 2017, 2019 & 2020 in Fig 4)

- Shallow firn ($z < 15$ m): $\Delta \rho_{RMS} \sim 4-12$ kg/m³ → $\Delta n_{RMS}/n \sim 0.01-0.035$
- Deep firn ($z > 15$ m): $\Delta \rho_{RMS} < 4$ kg/m³, $\Delta n_{RMS}/n < 0.01$



In-ice Radio Signal Modulation

Objective: Simulate RF Propagation from a deep source ($0, z_{TX}$) to receivers (x_{RX}, z_{RX}) using $n(z)$ profiles for different months and years at Summit → Quantify variation in RF signal due to changes in firn properties!

- RF Simulation codes:** MEEP (FDTD solution of Maxwell's equations) [7], paraProp (Parabolic Equation)[8], and NuRadioMC (ray tracing) [11] → **Output:** Electric field trace at RX positions: $E_{RX}(t)$ [V/m]
- TX/Source:** (example used: $z_{TX} = 500$ m) vertically-polarized dipole source emits band-limited impulse (0.08-0.3 GHz)
- Receivers (RX)** sample the signal at $z_{RX} : 0$ m to 200 m & $x_{RX} : 400$ m to 980 (see fig. 5)
- Analysis parameters:** Peak amplitude $E_{RX,max}$ [V/m], $\Delta t_{DR} = t_R - t_D$ [ns], fluence $\phi^E = \epsilon c \int E_{RX}(t)^2 dt$ [eV/m²]

Variation of parameter x at different times (and n -profiles), defined using residuals relative to mean \bar{x}

→ $\Delta x/\bar{x} = |x - \bar{x}|/\bar{x}$

Results:

Direct and Reflected/Refracted Paths (fig. 6):

- Two possible paths from TX to RX: direct & reflected or refracted (D & R_i)
- Only the R_r-path or R_f-paths traverse through the shallow firn layer

R-signal traces at $z_{RX} = 100$ m and $z_{RX} = 200$ m, June 2017, 2019 & 2020 (fig 6)

- R-signal $\Delta E_{max}/E_{max} < \sim 0.24$ at 100 m & 200 m (paraProp)
- R-signal $\Delta t_{DR} < \sim 22$ ns at 100 m & 200 m (paraProp)

Fluence variation between June 2017 and June 2019, for all receivers (fig.5)

- Variation increases at shallow depths & with distance from RX (paraProp)
- Fluence at 100 m & 200 m modelled with paraProp and MEEP (fig 8)

Fig.6 Paths of direct, reflected and refracted signals from 500 m source to RX at 100 m and 200 m (calculated with NuRadioMC)

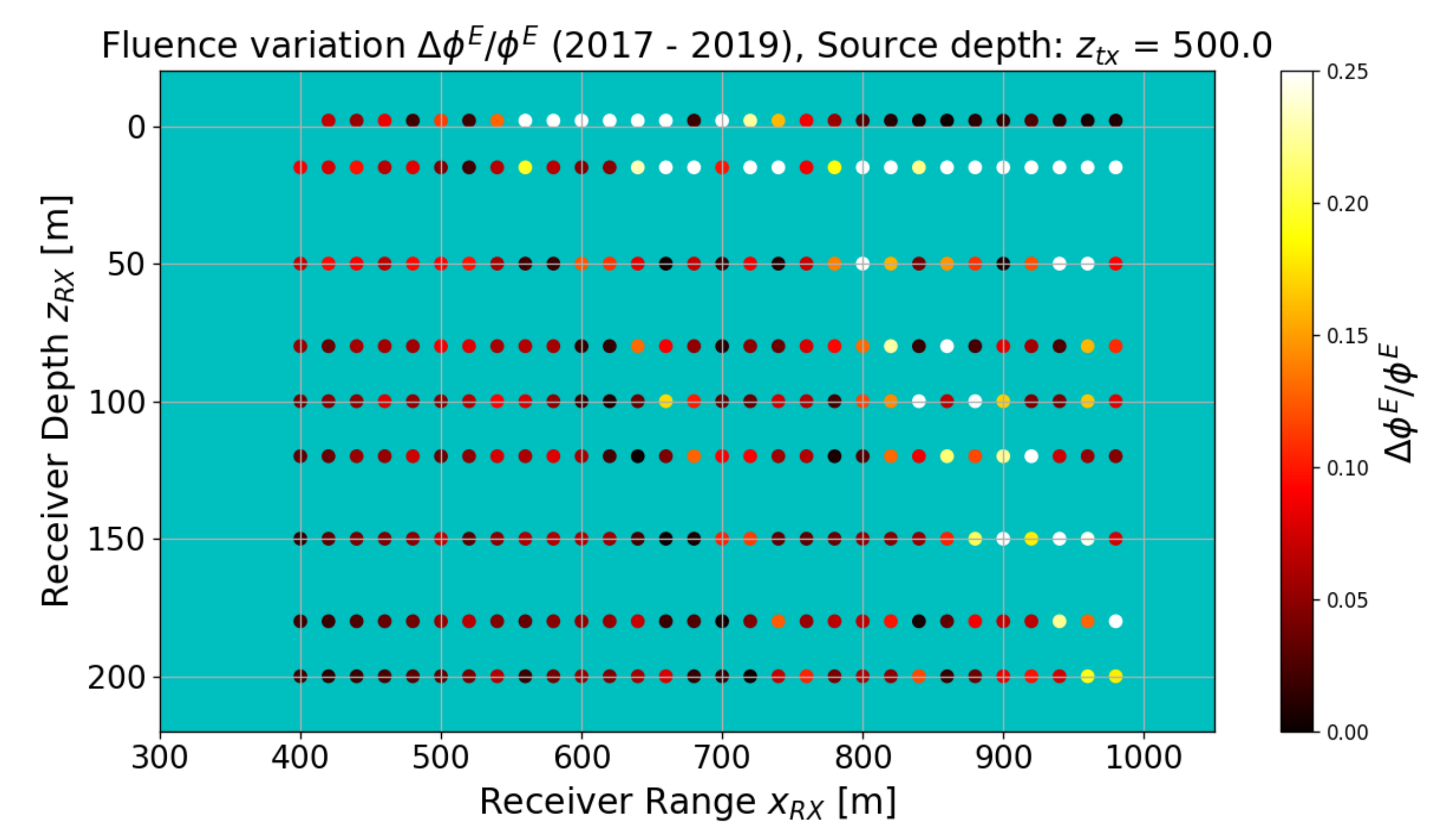
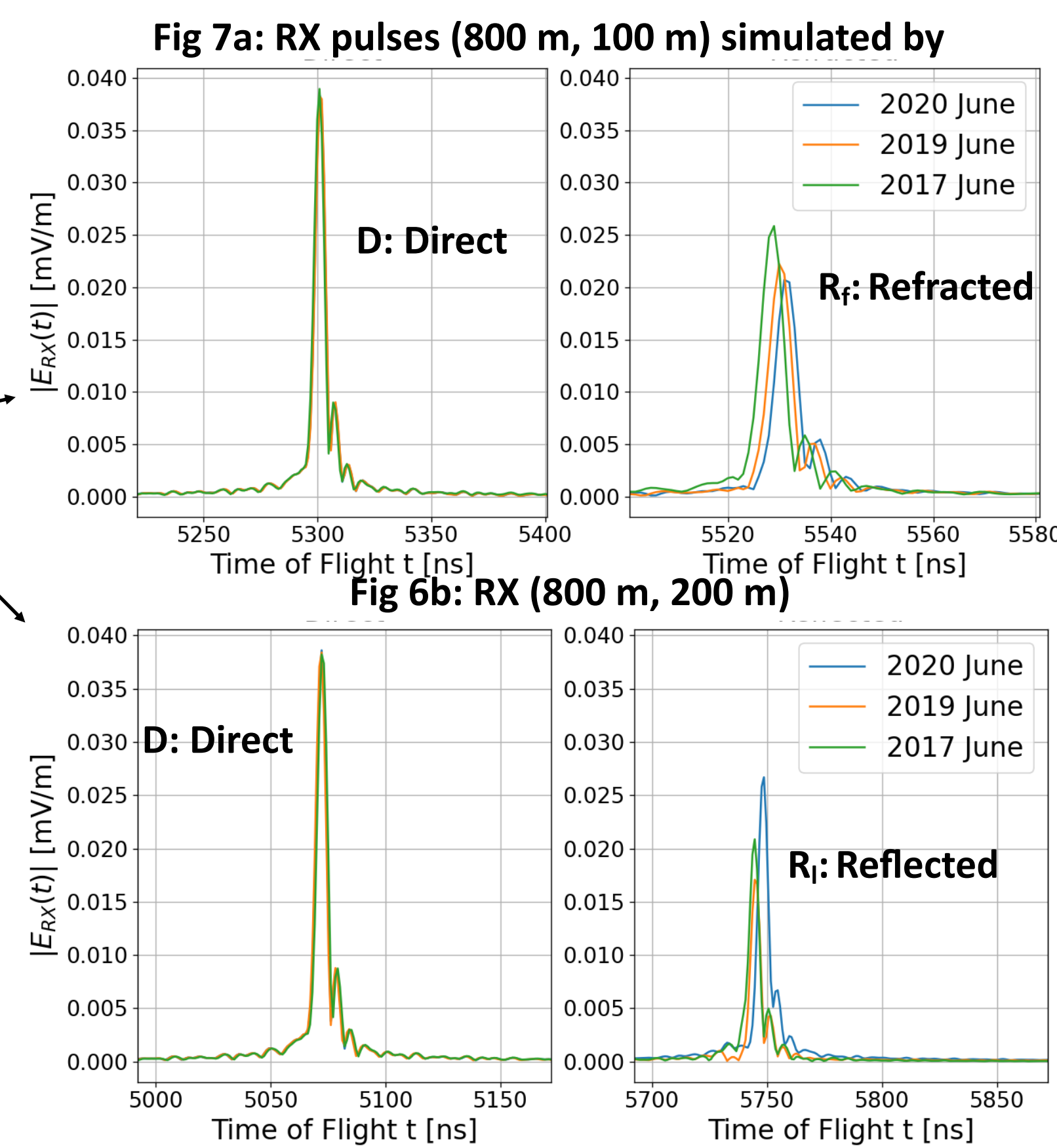
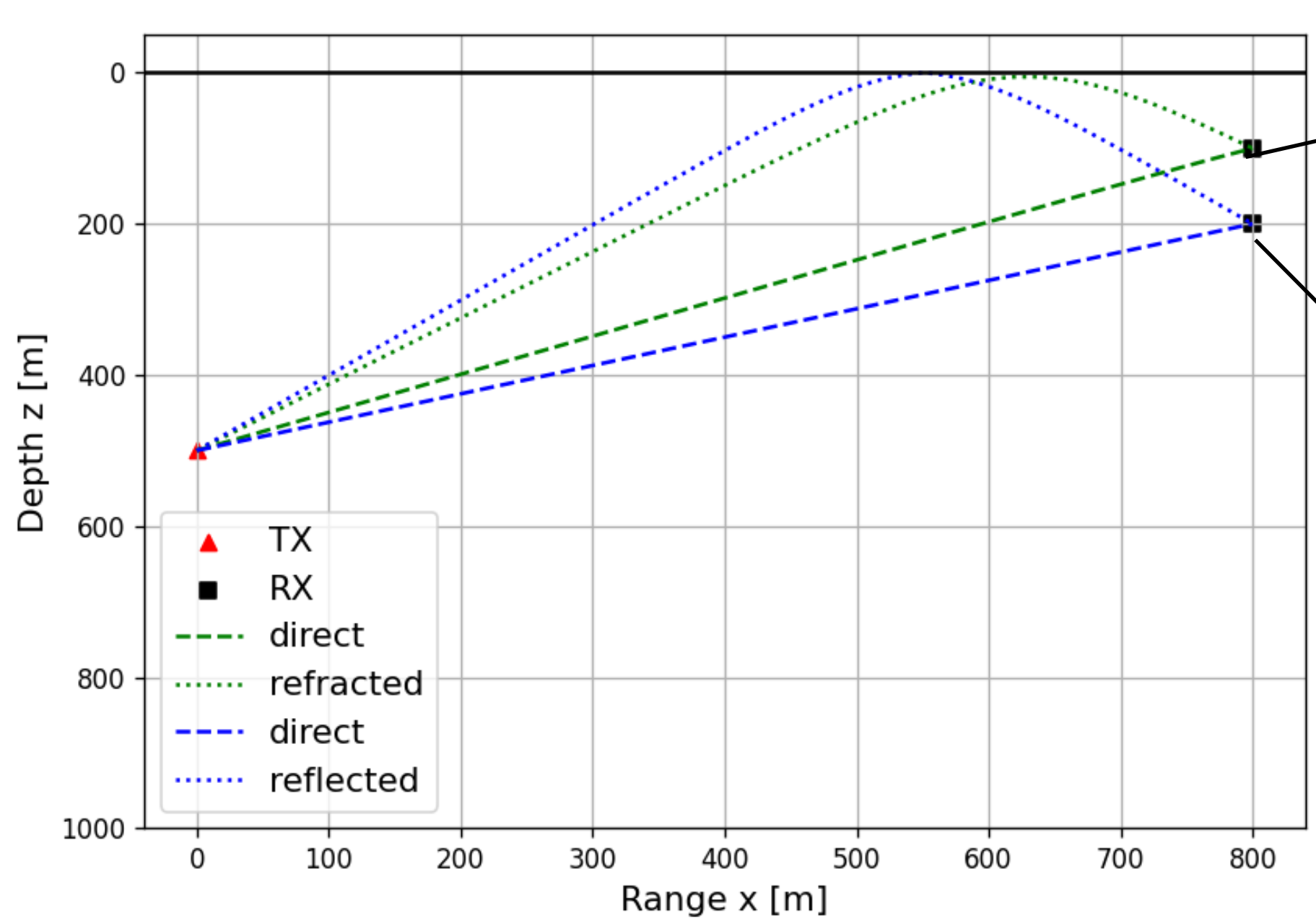


Fig.5 Fluence residuals in pulses at RX positions June 2017—June 2019 (paraProp)

Implications for Neutrino Reconstruction

Electric field fluence Φ^E is a reconstruction parameter for UHE-ν energy E_{ν} [5]:

$$\Phi^E \propto \sqrt{E_{\nu}} e^{-L/L_{\alpha}} e^{-\frac{|\theta - \theta_c|^2}{2\sigma_{\theta}}}$$

For each month from 2015 to 2020 we find the variation in fluence (Fig. 8):

- paraProp: $\Delta \Phi^E_R / \Phi^E_R > \sim 0.1$ ($x > 600$ m), $\sim 10^{-3} < \Delta \Phi^E_D / \Phi^E_D < \sim 10^{-2}$
- MEEP: $\Delta \Phi^E_R / \Phi^E_R > \sim 0.1$ ($x > 700$ m), $\sim 10^{-2} < \Delta \Phi^E_D / \Phi^E_D < \sim 10^{-1}$ ($x > 800$ m)

Preliminary finding: Under likely signal geometries, shallow firn fluctuations produce systematic uncertainty in the fluence of R-signals, and possibly for neutrino energy reconstruction as well

The polar regions are warming rapidly: understanding firn evolution and its modulation of Askaryan and Radar-Echo signals will be important for UHE-ν searches

References

- Askaryan Zh. Ekso. Teor. Fiz 41 (1961) 616
- Prohira et al. Phys Rev. D. 104 (2021)
- Stevens et al, Geosci. Model Dev., 13, 4355–4377, 2020
- Aguilar et al. Journal of Glaciology (2022)
- Aguilar et al. Eur.Phys.J.C 82 (2022) 2, 147
- Kovacs et al. (1995), Cold Regions Science and Technology
- Oskooi et al (2010), Com. Phys. Comm.
- Prohira et al. (2022), Instrumentation & Methods for Astrophys.
- Aguilar et al. (2023), Instrumentation & Methods for Astrophys.
- Allison et al. (2011), Instrumentation & Methods for Astrophys.
- Glaser et al. (2019), Instrumentation & Methods for Astrophys.
- Herron & Langwey (1980) J. Glaciology 25
- Prohira, de Vries et al. (2019) Phys. Rev. Lett. 124
- Frikken, (2023) Proceedings of Science (ICRC)

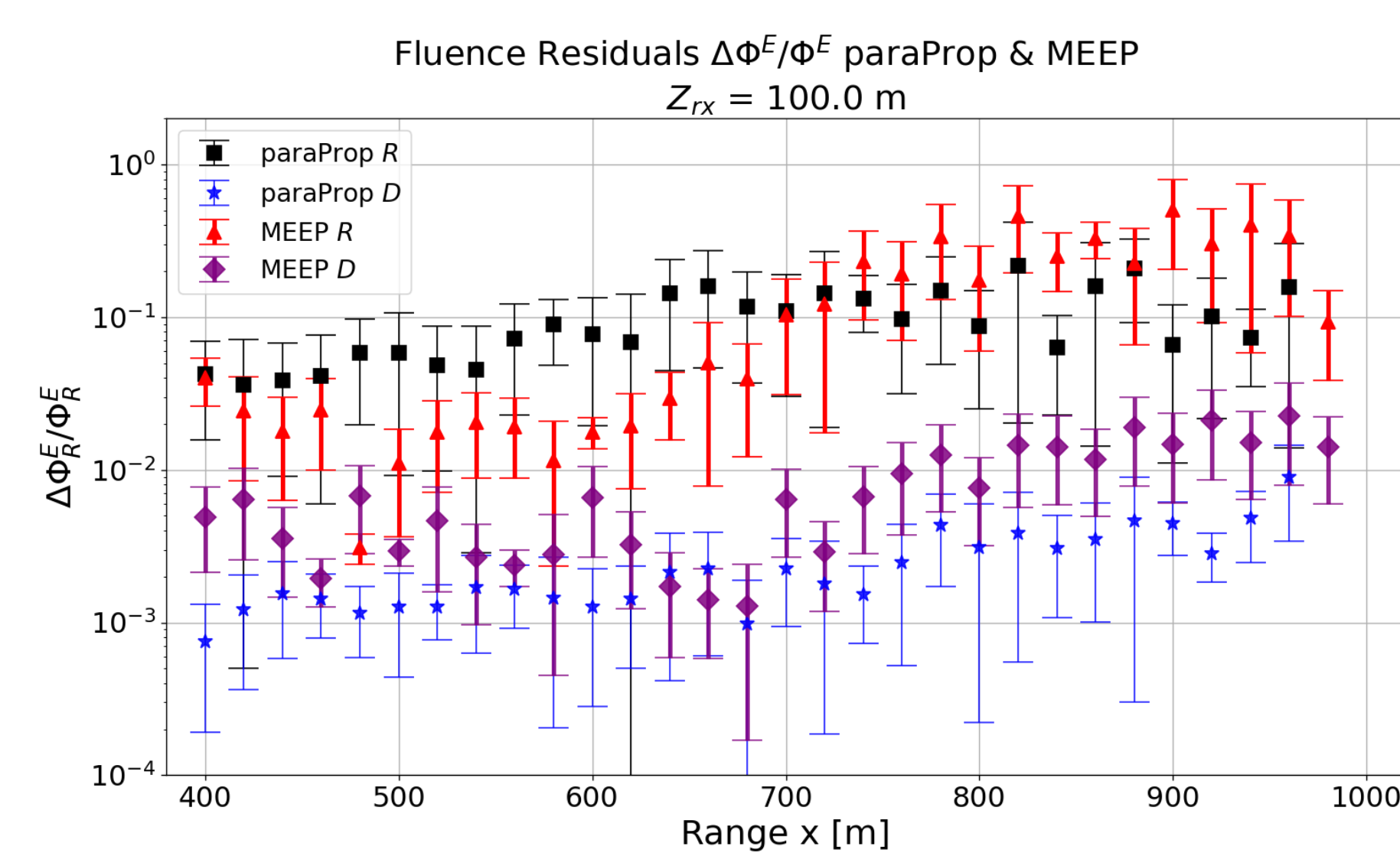


Fig.8 Φ^E residuals for CFM calculated profiles according to MEEP and paraProp: $n(z)$ profiles between 2015 & 2020